Received: October 17, 2024. Revised: November 5, 2024. 

INASS

*International Journal of*
Intelligent Engineering & Systems

http://www.inass.org/

# Design and Optimization of Vivaldi Antennas for Enhanced Breast Cancer Detection

**Azize Bhaij[1]*** **Abderrahim haddad[1]** **Redouane jouali[2]** **Khalid Sabri[1]**
**Mohssin Aoutoul[1]**

[1]*Laboratory of Information and Communication Sciences and Technologies, Department of Physics, University of Chouaib Doukkali, El Jadida, Morocco*
[2]*Laboratory of Information Technologies, National School of Applied Sciences, University of Chouaib Doukkali, El jadida, Morocco*
* Corresponding author's Email: bhaij.a@ucd.ac.ma

**Abstract:** Breast cancer remains a significant health challenge, with traditional detection methods such as mammography, ultrasound and Magnetic Resonance Imaging (MRI) exhibiting limitations in sensitivity and accessibility. This study investigates the design and optimization of Vivaldi antennas for ultra-wideband (UWB) microwave imaging to enhance breast cancer detection capabilities. Vivaldi antennas are recognized for their broad frequency coverage, effective impedance matching, and high radiation efficiency. Utilizing the Gibson method and CST Microwave Studio (CSTMWS), a Vivaldi antenna was fabricated on an FR4 substrate, achieving dimensions of 52.45 × 53 mm². Experimental and simulated results demonstrate excellent performance in terms of return loss, gain, and radiation efficiency across a frequency range of 2.55 GHz to 10.23 GHz. The findings suggest that integrating advanced Vivaldi antenna technology into breast cancer detection systems can significantly improve early diagnosis and patient outcomes, providing a non-invasive and accurate detection method for this critical health issue.

**Keywords:** Breast cancer detection, Vivaldi antennas, Ultra-wideband, Microwave imaging, Medical applications, Impedance matching, Radiation efficiency, Non-invasive detection, Antenna design, Signal processing.

## 1. Introduction

Breast Breast cancer is a leading health issue for women, accounting for 32% of new cancer cases in the U.S. in 2024. With 310,720 new cases expected and a lifetime risk of 13% for women, it remains a major concern. Breast cancer is projected to cause 42,250 deaths this year, making it a significant cause of cancer-related mortality [1]. These figures highlight the critical importance of early detection and effective treatments to improve patient outcomes [2-4]. While traditional breast cancer detection methods such as mammography [5, 6], ultrasound [7-9], and MRI [10-12] are widely used, they have notable limitations. For example, mammography often faces sensitivity challenges, especially in women with dense breast tissue, which can lead to false negatives. Additionally, exposure to ionizing radiation remains a concern. Although ultrasound and MRI are non-invasive, they may lack specificity and accessibility, potentially leading to unnecessary biopsies or high costs.

In response to these challenges, there has been growing interest in developing advanced detection technologies, particularly in the field of microwave imaging using UWB antennas [13-15]. Vivaldi antennas, operating within the UWB range of 3.1 to 10.6 GHz according to Federal Communications Commission (FCC) requirements [16, 17], are valued for their broad bandwidth, high gain, and versatility. They are particularly essential in medical imaging for radar-based breast cancer detection, where they significantly improve image resolution and tissue penetration [18-20] .This advantage is crucial for early detection, as the wide frequency range of Vivaldi antennas allows for the detection of subtle

Received: October 17, 2024. Revised: November 5, 2024. 

tissue changes associated with cancerous growths [21, 22]. Additionally, these antennas play a key role in other fields, such as ground-penetrating radar for precise subsurface exploration [23], UWB communication networks including future 5G technologies [24, 25], and through-wall imaging, military radar systems and radio astronomy due to their wideband capabilities [26].

Among the various antenna designs explored for breast cancer detection[27], the Vivaldi antenna stands out as a promising candidate due to its inherent wideband capabilities, excellent impedance matching, and high radiation efficiency. The tapered slot structure of the Vivaldi antenna allows it to cover a broad frequency range while maintaining a compact design and efficient radiation properties. Variants of Vivaldi antennas include antipodal Vivaldi antennas [28], tapered slot antennas[29], side-slotted Vivaldi antennas[30], and corrugated Vivaldi antennas[31]. Additionally, there have been developments of dielectric lens Vivaldi antennas[20], flexible Vivaldi antennas[32], U-shaped slot Vivaldi antennas[33], and parasitic-element Vivaldi antennas [26].

This study focuses on the design and optimization of a novel Vivaldi Trapezoidal-Ellipse UWB Antenna specifically dedicated to breast cancer detection, utilizing the Gibson method[29], which incorporates an exponential profile for the radiating element. The objective of this study is to enhance the antenna's performance in terms of bandwidth, directivity, and return loss. The proposed Vivaldi Trapezoidal-Ellipse Antenna, fabricated on an FR4 substrate, features a trapezoidal rectangular feed line with an elliptical head and an exponentially tapered radiating structure with a rectangular slot at its end, accompanied by four elliptical slots. This design is specifically intended to achieve effective impedance matching across a wide frequency range. The geometric configuration and optimization process resulted in an antenna with dimensions of 52.45 × 53 mm². Experimental and simulated results demonstrate that the proposed Vivaldi antenna exhibits exceptional performance in terms of return loss, gain, and radiation efficiency, establishing it as a highly effective tool for breast cancer detection.

This research is organized as follows: Section 2 presents the theoretical design and materials used for the Vivaldi antenna. Section 3 details the design and optimization stages of the antenna. Section 4 discusses the experimental and simulated results with an in-depth performance evaluation. Finally, Section 5 concludes the study and offers suggestions for future research directions.

## 2. Theoretical design and methodology

### 2.1 Theoretical construction of a vivaldi antenna

Vivaldi antennas are wideband antennas characterized by their tapered slot structure, widely used for their broad frequency coverage, good impedance matching, and high radiation efficiency. The Gibson method, a well-known approach for designing these antennas, relies on an exponential profile for the radiating section, allowing for a gradual transition between the feed line and free space. This design minimizes reflections and maximizes radiation efficiency [29].

Exponential Profile:

$$Y(x) = \pm y_0 e^{kx} \tag{1}$$

Where y is the width of the antenna at a distance x, $y_0$ is the initial width, and k is the exponential growth coefficient.

### 2.2 Vivaldi antenna design

The PVA, as shown in Fig. 1, is designed to

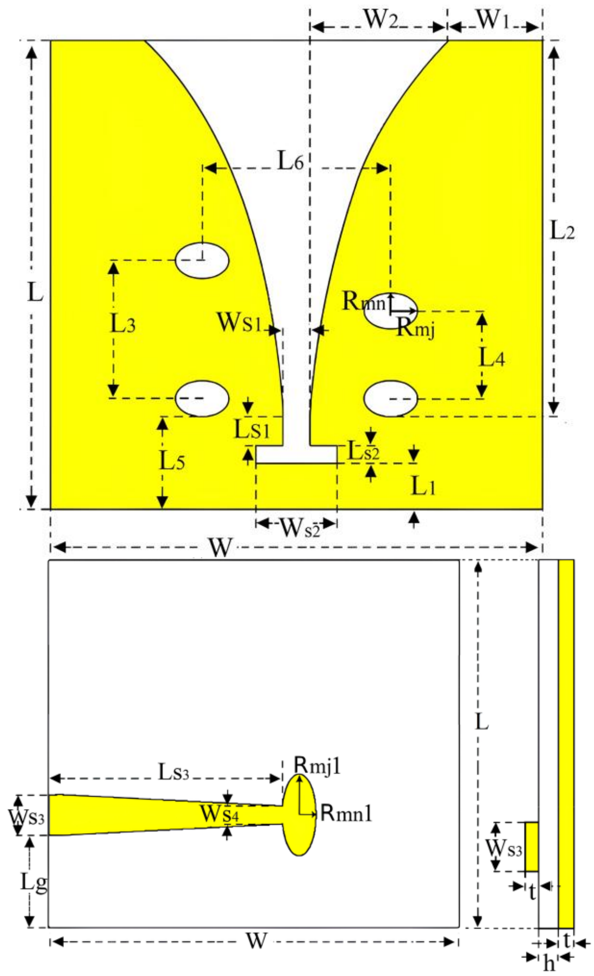


Figure. 1 Front and Side View of the PVA

Table 1. Parameter Names and Values for the PVA

| Parameter | Value(mm) | Parameter | Value(mm) |
|---|---|---|---|
| L | 52.45 | Rmj1 | 2 |
| W | 53 | Rmn1 | 0.9 |
| Ls1 | 3.174 | W1 | 20.46 |
| Ws1 | 0.986 | W2 | 5.54 |
| Ls2 | 8.9 | Lg | 8.495 |
| Ws2 | 1.4 | L1 | 6.825 |
| Ls3 | 29.18 | L2 | 42.45 |
| Ws3 | 2 | L3 | 23 |
| Ws4 | 0.5 | L4 | 3 |
| Rmj | 0.9 | L5 | 8.325 |
| Rmn | 0.89 | L6 | 8.6 |

achieve wideband performance suitable for breastcancer detection. It is fabricated on an FR4 substrate with the following specifications: a thickness of 1.6 mm, a relative permittivity (εr) of 4.3, and a loss tangent of 0.035. The overall dimensions of the antenna measure 52.45 × 53 mm², optimized to balance performance and compactness.

The design features a trapezoidal rectangular feed line coupled with an exponentially tapered slot, which functions as the radiating element. This tapering profile is essential for ensuring a smooth transition from the feed line to free space, thereby minimizing reflections and maximizing radiation efficiency. The final dimensions of the antenna, as detailed in Table 1, were optimized using CSTMWS.

In our application, the exponential taper of the Vivaldi antenna is defined by the following equation:

- **Y(x):** Width of the antenna at position x.
- $y_0$: Initial width $y_0 = \pm \frac{w_{s_1}}{2}$
- K: Exponential growth coefficient, calculated as $k = \frac{ft}{10^3}$
- X: Position along the length $L_2$

Consequently, the equation for the exponential curve can be expressed as follows:

$$Y(x) = \pm \frac{w_{s1}}{2} e^{\frac{ft*x}{1000}} \tag{2}$$

### 2.3 Design and optimization stages of the vivaldi antenna

The design process required the use of CSTMWS to simulate and optimize the antenna's performance. The simulation focused on key parameters such as reflection coefficient (S11), gain, and radiation efficiency within the desired frequency range, spanning from 2.55 GHz to 10.23 GHz. Several design iterations were conducted to optimize these parameters. The steps, illustrated in Fig. 2, include analyzing the dimensions of the feed line, adding an ellipse to its end, incorporating complementary structures such as rectangular slots, and inserting two symmetrical elliptical slots after two offset elliptical slots.

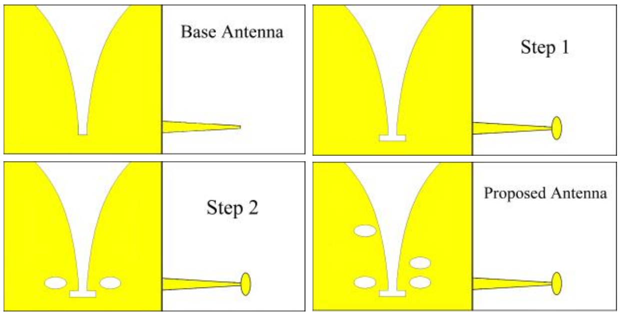


Figure. 2 Design and Optimization Steps for the PVA

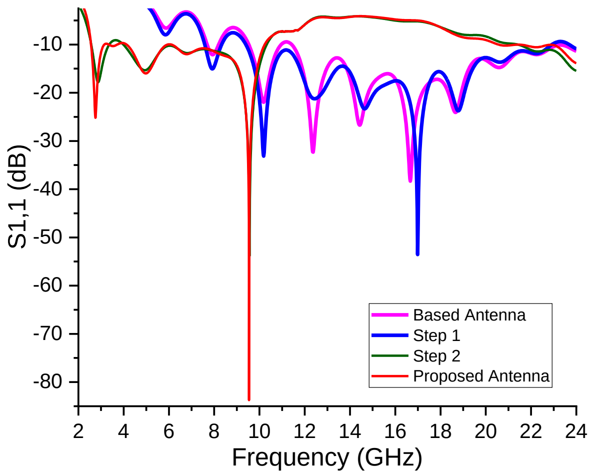


Figure. 3 S11 Parameter Comparison of Based Antenna, Step 1, Step 2, and Proposed Antenna Designs

The results presented in Fig. 3 show a comparison of performance in terms of the S11 between the basic antenna and the various modification stages (Step 1 and Step 2) leading to the proposed antenna. The basic model exhibits wideband characteristics ranging from 9 to 23 GHz but does not meet the requirements set by the FCC for medical applications. To improve performance, a rectangular slot was added in the front view, as well as an ellipse in the side view, at the end of the feed line during Step 1. This modification resulted in a notable improvement in impedance, although the bandwidth remained unchanged. Step 2, which includes the addition of two symmetrical slots in the front view, led to a shift and reduction in bandwidth, decreasing from 13.6 GHz (from 9.35 to 22.95 GHz) to 7.76 GHz (from 2.55 to 10.23 GHz), while also improving performance in terms of the S11.Finally, the

Received: October 17, 2024. Revised: November 5, 2024. 

proposed antenna, optimized by the insertion of two additional elliptical slots in the front view, demonstrates Significantly superior performance, with a greatly improved S11 and an optimal bandwidth ranging from 2.55 GHz to 10.23 GHz. This optimization makes the antenna particularly suitable for communication applications and detection systems, notably for breast cancer detection.

## 2.4 Parametric analysis and design modifications

### 2.4.1. Impact of trapezoidal feed line dimensions (Width Ws3 and Ws4) on antenna performance

The Fig. 4 shows the S11 parameter as a function of frequency for an antenna with a trapezoidal rectangular feed line, where the upper height is designated as Ws3 and the lower base as Ws4. The first figure illustrates the variation of Ws3 (2 mm, 2.3 mm, and 2.6 mm), demonstrating that all three configurations have a bandwidth ranging from 7.584 to 23 GHz, with significant dips around 10.18 GHz

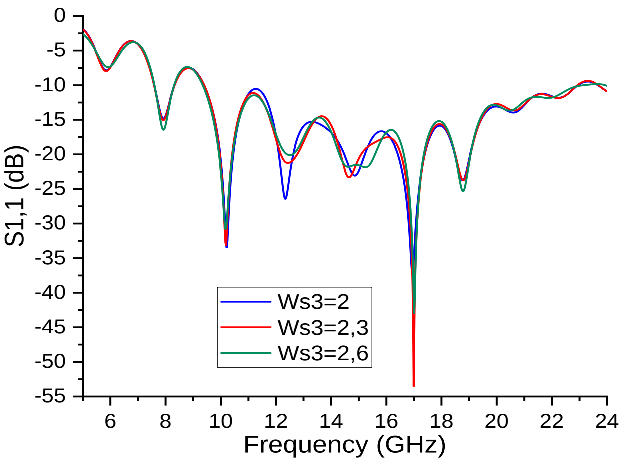


(a)

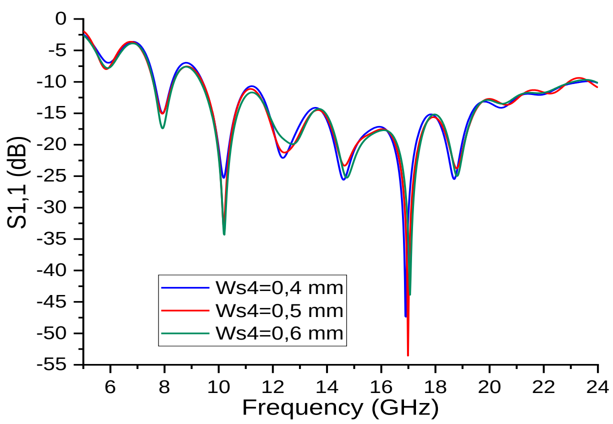


(b)

Figure. 4 Return Loss of Trapezoidal Rectangular Feed Line Antenna with Variations in Ws3 and Ws4

and 16.98 GHz, indicating good impedance matching. The second figure presents the variations of Ws4 (0.4 mm, 0.5 mm, and 0.6 mm), also showing the same bandwidth and significant dips at the same frequencies. Although the differences between the curves are minimal, the configurations with Ws3 = 2.6 mm and Ws4 = 0.4 mm tend to exhibit slightly better impedance matching at certain frequencies.

### 2.4.2. Effect of inserting the rectangular slot and the ellipse in the feed line on antenna performance

The Fig. 5 shows the S11 parameter as a function of frequency for a modified Vivaldi antenna designed for breast cancer detection. The modification includes adding a rectangular slot with dimensions (ls2, ws2) and an ellipse with dimensions (Rmj1 and Rmn1) in the trapezoidal rectangular feed line. The results indicate a bandwidth ranging from 2.55 to 10.23 GHz, with a significant dip around 2.75 GHz and another pronounced dip around 9.54 GHz, reaching approximately -53 dB, suggesting excellent impedance matching at these frequencies.

Compared to step 4, where the antenna lacked both the ellipse in the trapezoidal rectangular feed line and the rectangular slot, this new modification improves the response by reducing reflection losses while narrowing the bandwidth from 15 GHz to 7.5 GHz. These adjustments optimize the antenna's efficiency and selectivity for medical detection applications, particularly for breast cancer detection.

### 2.4.3. Impact of inserting elliptical slots on the performance of the PVA.

The Fig. 6 Shows the S11 parameter as a function of frequency for a Vivaldi antenna with two different configurations: one with two elliptical slots and the other with four elliptical slots. Comparing the two

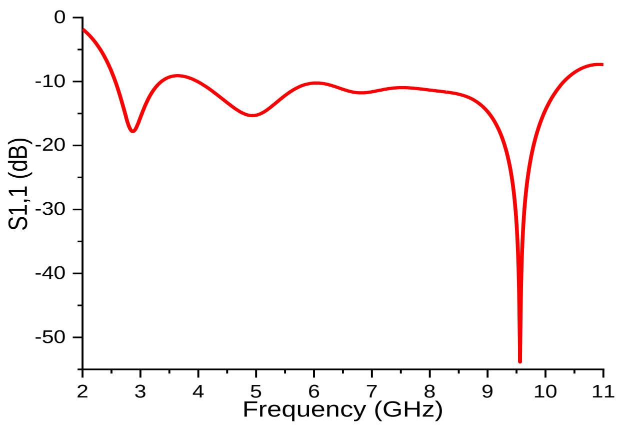


Figure. 5 Return Loss of Modified Vivaldi Antenna with Rectangular Slot and Elliptical Feed Line

 DOI: 10.22266/ijies2025.0229.28

Received: October 17, 2024. Revised: November 5, 2024. 

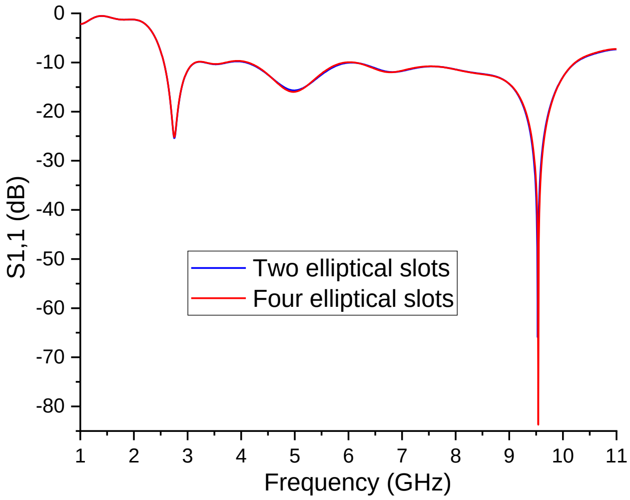


Figure. 6 Comparison of the PVA with Two and Four Elliptical Slots

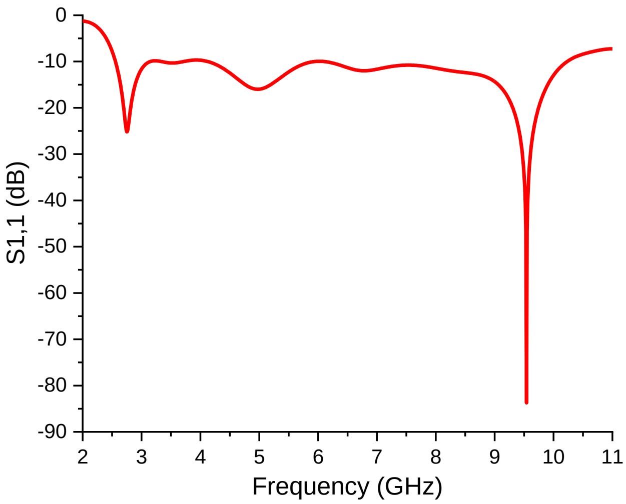


Figure. 7 S11 Parameter Characterization of the PVA

configurations, the return loss S11 curve for the two elliptical slots (blue curve) shows a significant dip around 2.75 GHz, indicating good impedance matching at this frequency. There are also smaller dips around 5 GHz and a very deep dip of -65 dB around 9.54 GHz, indicating excellent impedance matching at these frequencies. The S11 curve for the four elliptical slots (red curve) is very similar to that of the two elliptical slots, showing a significant dip around 2.75 GHz and similar dips around 5 GHz and 9.54 GHz. The main difference is that the four elliptical slot configuration tends to have deeper dips, reaching -83.71 dB at 9.54 GHz, indicating slightly better impedance matching. In conclusion, the Vivaldi antenna performs well with both two and four elliptical slot configurations, exhibiting multiple resonant frequencies in the range of 2.55 GHz to 10.23 GHz. The four elliptical slot configuration offers better impedance matching, making it a potentially more efficient design for applications requiring minimal return loss.

### 2.5 Simulation results and analysis of the PVA

#### 2.5.1. Return loss of a PVA

The antenna results, illustrated in Fig. 7, reveal notable performance with two key resonance frequencies at 2.75 GHz and 9.54 GHz, corresponding to S11 values of approximately -25 dB and -83.73 dB, respectively, indicating excellent impedance matching. The antenna operates effectively across a frequency range from 2.55 GHz to 10.23 GHz, demonstrating reasonable performance with low return loss throughout this bandwidth. These characteristics make the antenna well-suited for applications that demand reliable performance at the specified frequencies.

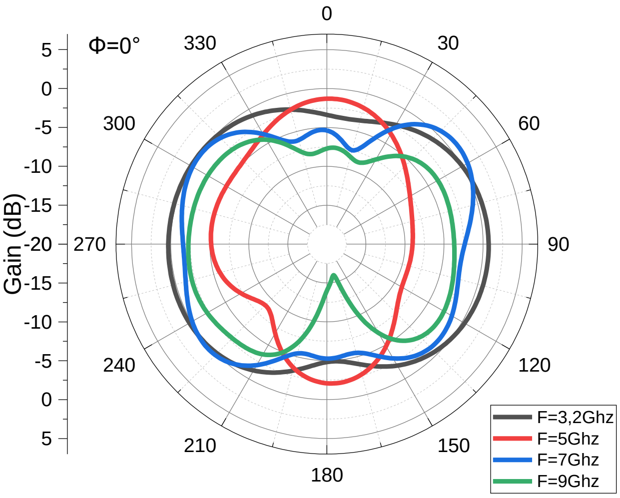


(a)

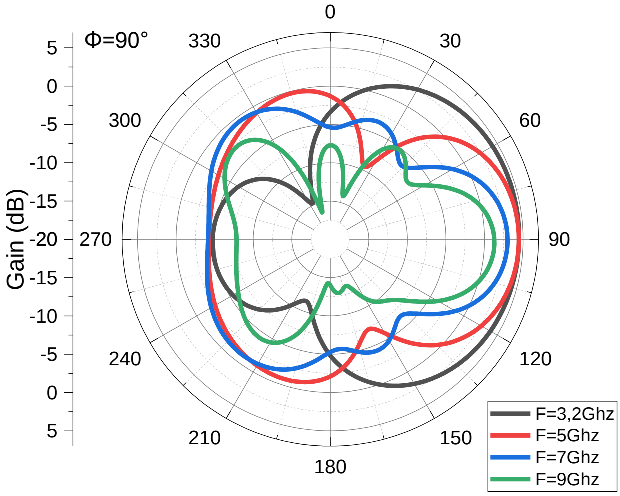


(b)

Figure. 8 Radiation Patterns of a PVA at Different Frequencies for: (a) Φ = 0° and (b) Φ = 90°

 DOI: 10.22266/ijies2025.0229.28

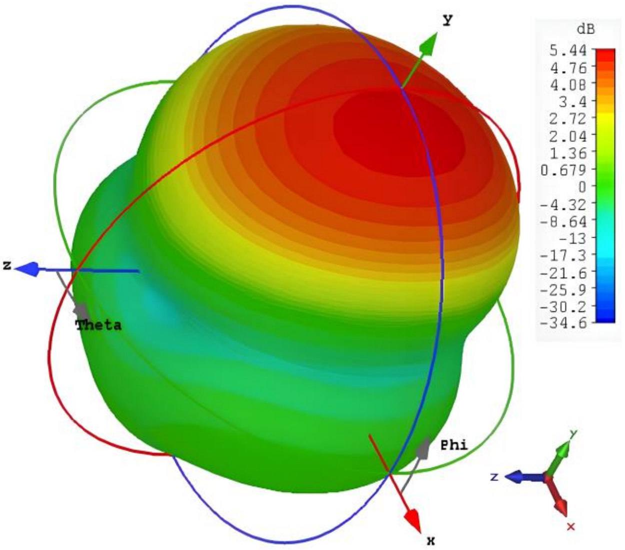


Figure. 9 3D Radiation Patterns of the Antenna with Gain Distribution

### 2.5.2. Radiation patterns of a PVA

Fig. 8 illustrate the radiation patterns of the Vivaldi antenna at different frequencies (3.2, 5, 7, and 9 GHz) for phi angles of 90 degrees and 0 degrees, respectively. At $\Phi = 90°$, the gain is uniformly distributed at 3 GHz but becomes more directional at higher frequencies. Conversely, at $\Phi = 0°$, the radiation pattern is broad and symmetrical at 3 GHz, then demonstrates increased directionality as the frequency rises. These findings indicate that the Vivaldi antenna exhibits variable directionality and complex radiation behavior depending on the frequency and phi angle, making it suitable for applications that require precise directionality.

### 2.5.3. Maximum gain (dB) of a PVA

The Fig. 10 illustrates the maximum gain (dB) as a function of frequency for the PVA. Spanning a frequency range from 2.55 GHz to 10.23 GHz, the graph highlights the antenna's performance across this wide spectrum. The gain begins to rise from 2.55 GHz, peaking at approximately 5.5 GHz with a maximum gain of about 5.6 db. Between 3 GHz and 9 GHz, the gain remains relatively high, fluctuating between 2.5 dB and 5.6 dB, which indicates robust performance in this range. Beyond 9 GHz, the gain gradually declines, reaching approximately 2.26 dB at 10.23 GHz. Overall, the PVA demonstrates commendable performance in terms of maximum gain within the 3 GHz to 10 GHz range, making it well-suited for applications that require high gain in this frequency band.

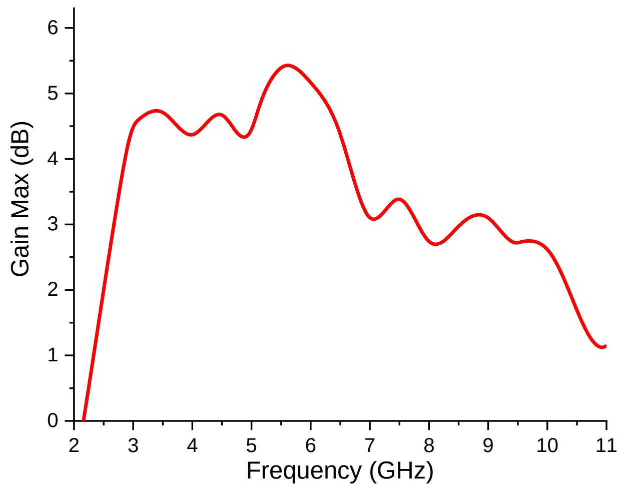


Figure. 10 Maximum Gain (dB) of a PVA

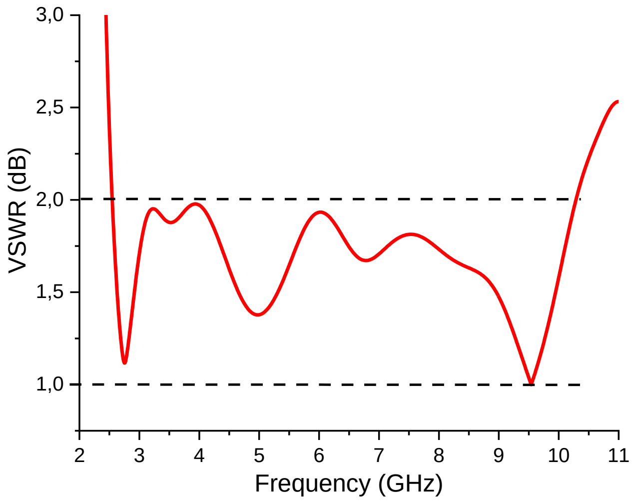


Figure. 11 VSWR (dB) of a PVA

### 2.5.4. Voltage standing wave ratio analysis of a PVA

The Fig. 11 shows the VSWR as a function of frequency for a PVA. Between 2.55 GHz and 10.28 GHz, the VSWR oscillates between 1 and 2, indicating variations in the quality of impedance matching. Around 9.54 GHz, the VSWR reaches a significant dip, very close to 1, suggesting excellent impedance matching. Beyond 10.28 GHz, the VSWR increases rapidly, exceeding 2, indicating a decrease in the quality of the matching. These results show that the PVA is well-suited for frequencies around 2.55 GHz and 10.28 GHz, but presents less effective matching outside these ranges.

### 2.5.5. Radiation efficiency of a PVA

The Fig. 12 shows the radiation efficiency (η) as a function of frequency for a PVA. The radiation efficiency starts at just over 1.09 at 2.5 GHz,

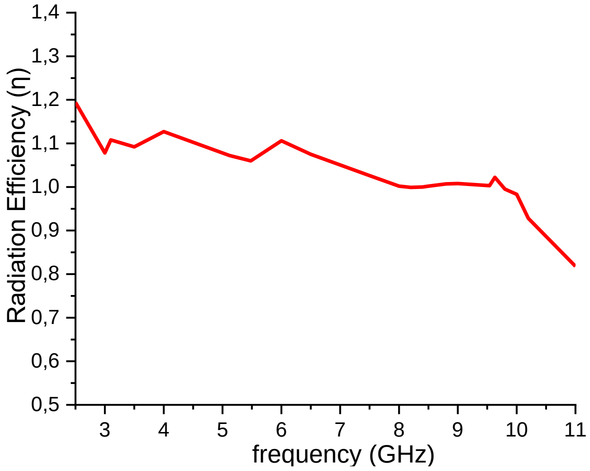

Figure. 12 Radiation Efficiency (η) of a PVA

indicating an efficiency slightly above 100%, which may be due to measurement errors or specific conditions of the antenna. Between 3 GHz and 9.63 GHz, the efficiency varies slightly but remains close to 1, indicating good radiation efficiency in this frequency range. After 9.63 GHz, the efficiency begins to decrease gradually, reaching around 0.9 at 10 GHz. Beyond 10 GHz, the radiation efficiency decreases more rapidly, reaching about 0.8 at 11 GHz. These results show that the PVA offers good radiation efficiency between 3 GHz and 9.63 GHz, but the efficiency decreases at higher frequencies, which could limit the antenna's performance in these higher frequency ranges.

**2.5.6. Comparison of vivaldi antenna designs with other antennas in the literature**

The comparison of antenna designs reveals significant differences in terms of bandwidth, resonant frequency, gain, dimensions, substrates, slot types, complexity, and applications. The Trapezoidal-Ellipse Vivaldi antenna stands out with a wide bandwidth ranging from 2.55 to 10.23 GHz, with resonant frequencies at 2.75 GHz and 9.54 GHz, which are essential for early detection of tissue abnormalities. Its minimal S11 of -83 dB ensures excellent impedance matching and efficient power transmission. Unlike other complex designs that use U-shaped slots or Defected Ground Structures (DGS), this antenna remains simple with its rectangular and elliptical slots, reducing performance variability and facilitating fabrication while maintaining a compact size (52.45 × 53 mm²).

Other antenna designs have their pros and cons. For example, antenna [34] covers a broader bandwidth but has a more complex structure with parasitic elements. Antenna [30] offers higher gain, but its larger dimensions complicate integration into portable devices. As for antenna [33], while achieving a gain of 7 dB, it relies on dielectric lenses, increasing design complexity and manufacturing costs.

The proposed antenna uses the FR4 substrate, offering a good balance between cost and performance. Other substrates, such as the Rogers RT/duroid 5870 used in antenna[31], provide better thermal stability and lower dielectric losses but are more expensive. The Polyimide used in antenna [32] is suitable for portable devices but presents challenges in structural stability.

Table. 2 Comparison of Antenna Specifications and Performance Metrics

| Study | Proposed Design | [34] | [28] | [30] | [31] | [33] | [32] | [35] |
|---|---|---|---|---|---|---|---|---|
| BW (GHz) | 2.55 - 10.23 | 2.79 - 16.66 | 1.4 - 8 | 1.54-7 | 5 - 20 | 2.33-7.9 | 4 – 5.2 | 2.6 - 11.6 |
| RF (GHz) | 2.75, 9.54 | NR | NR | 1.79, 2.89, 5.81 | 5.1 | 4.036,5.88 | 4.4 | 5.2 |
| Min S11 (dB) | -83 | NR | NR | -NR | -39 | -51.74, -51 | -32 | -45 |
| Gain (dB) | 5.6 | 4.77 | 11.31 | 9.8 | 7 | 6.2 | 2.33 | 6.73 |
| Size (mm$^2$) | 52.45 × 53 | 45 × 40 | 50 × 86 | 88×75 | 48 × 60 | 55 × 65 | 25 × 20 | 42.85×42.85 |
| Substrate | FR4 | FR4 | FR4 | RT/duroid 5870 | FR4 | FR4 | Polyimide | FR4 |
| Type of Slots | Elliptical slots | Rectangular slots | Parasite, corrugation and dielectric lens | Without slot | slot edge | U-shaped slots | copper rectangles and slots (DGS) | Slits and Meandered Edge |
| Design | Simple | Medium | High | Medium | Medium | Medium | Medium | High |
| Application | Medical Imaging | Medical Imaging | Medical Imaging | Medical Imaging | Communication | Medical Imaging | Medical Imaging | Medical Imaging |

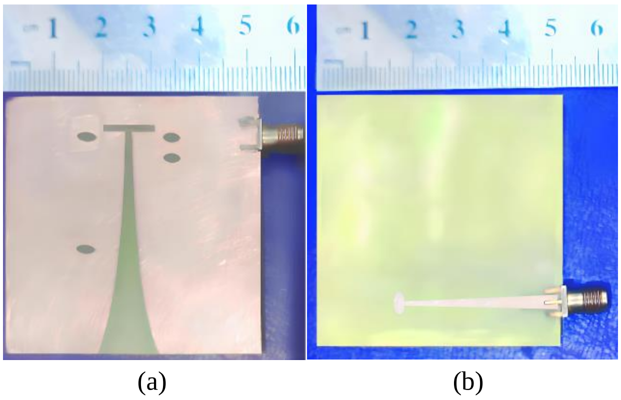


Figure. 13 Photograph of the fabricated prototype: (a) Top view and (b) bottom view

### 2.6 Experimental results

A prototype of the simulated UWB Vivaldi antenna has been fabricated, as illustrated in Fig. 13. It was made using an FR4 substrate with a permittivity of 4.3, a thickness of 1.6 mm, and a loss tangent of 0.035. The final structure measures 52.45 × 53 mm².

#### 2.6.1. Comparison of simulated and measured reflection coefficient for UWB vivaldi antenna

Fig. 14 illustrates the comparison between the simulated and measured results of the S11 over a frequency range from 2.55 GHz to 10.23 GHz. The simulated and measured curves show good agreement, particularly in the frequency ranges around 2.55 GHz and 10.23 GHz, where the antenna exhibits optimal impedance matching (S11 < -10 dB). These dips mark several resonant frequencies, indicating that the antenna is well-suited for UWB

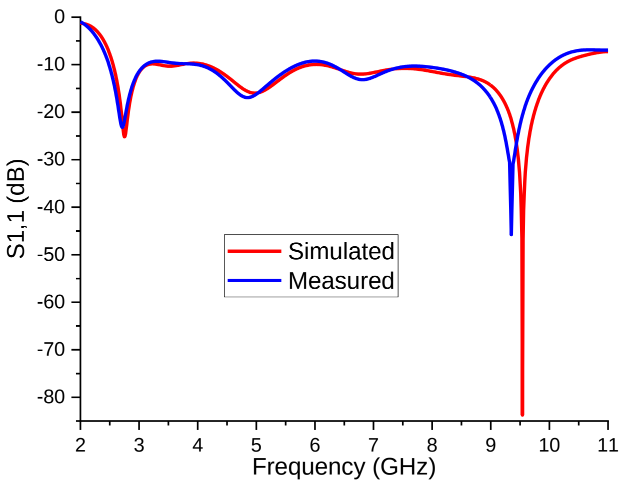


Figure. 14 Measured and simulated results of the return loss parameter of the PVA UWB

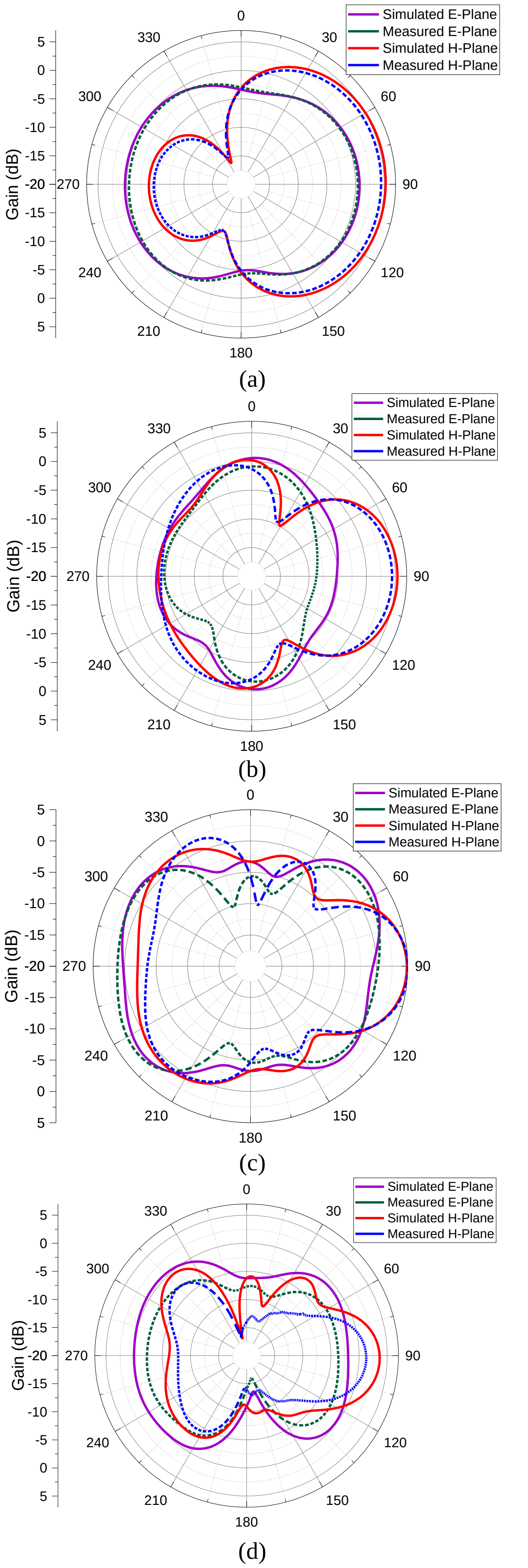


Figure. 15 Comparison of Simulated and Measured Radiation Patterns at: (a) 3.2 GHz, (b) 5 GHz, (c) 7 GHz, and (d) 9 GHz for E-plane (Φ = 0°) and H-plane (Φ = 90°)

applications. Despite some minor discrepancies between 5 GHz and 7 GHz, likely due to manufacturing tolerances or measurement inaccuracies, the two curves converge around 9.5 GHz with excellent alignment, reaching values as low as -50 dB, reflecting low reflection and good performance. This demonstrates a wide bandwidth and effective matching, thus validating the antenna design for practical applications.

#### 2.6.2. Analysis of radiation patterns and experimental validation of antenna performance

The simulated and measured radiation patterns, as shown in Fig. 15, exhibit good agreement overall, especially at the lower frequencies of 3.2 GHz and 5 GHz. However, as the frequency increases to 7 GHz and 9 GHz, more significant discrepancies arise, particularly in the side and back lobes. These differences may be attributed to manufacturing tolerances, variations in the measurement setup, or environmental factors.

#### 2.6.3. Comprehensive comparison between simulated and measured gain max

Fig. 16 shows a comparison between the simulated and measured Gain Max data over a frequency range from 2.55 to 10.23 GHz. Both curves follow a similar overall trend, indicating that the simulation accurately reflects the real measurements. However, notable discrepancies arise at higher frequencies, where the simulated gain tends to overestimate the measured values. These differences could stem from unmodeled physical phenomena in the simulation or minor inaccuracies in the measurements. Overall, the simulation provides a good approximation of real-world conditions, though further refinement could improve its accuracy, especially at higher frequencies.

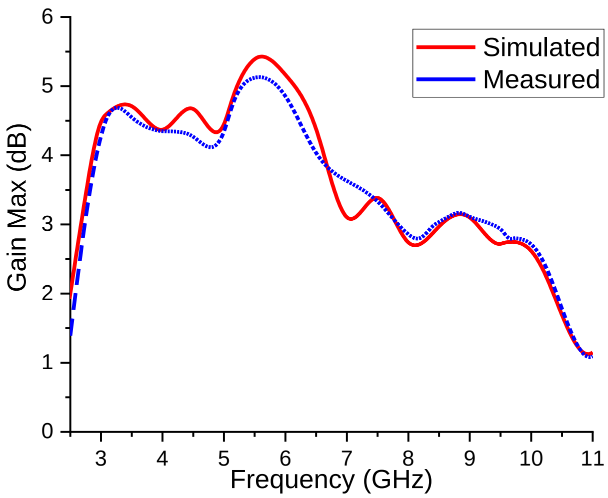


Figure. 16 Comparison of Simulated and Measured Gain Max Over Frequency Range

## 3. Conclusion

In conclusion, the Trapezoidal-Ellipse Vivaldi antenna strikes an optimal balance between gain, bandwidth, and structural simplicity, making it particularly well-suited for medical applications, especially breast cancer detection. By addressing the challenges of existing designs, this antenna offers a reliable and efficient solution for microwave medical imaging. This study has successfully demonstrated the design and optimization of Vivaldi antennas for UWB microwave imaging with a specific focus on breast cancer detection. The proposed antenna exhibits excellent performance characteristics, with experimental and simulated results confirming its effectiveness in terms of return loss, gain, and radiation efficiency. These findings highlight the antenna’s significant potential to enhance early breast cancer detection by providing a non-invasive, accurate, and accessible diagnostic method. Looking ahead, further refinements to the antenna design and exploration of its applications in other medical imaging fields are crucial. Additionally, establishing comprehensive guidelines for implementing Vivaldi antennas in clinical settings will be essential to fully leverage their potential in improving cancer detection and treatment. The integration of this advanced Vivaldi antenna technology promises a major step forward in non-invasive breast cancer diagnosis and patient outcomes.

## Conflicts of Interest

The authors declare no conflict of interest.

## Author Contributions

The conceptualization of this study was led by Azize Bhaij and Abderrahim Haddad, who also developed the methodology. Software development was carried out by Azize Bhaij. Validation was conducted by Azize Bhaij, Abderrahim Haddad, and Redouane Jouali. Formal analysis was performed by Azize Bhaij. Investigation was directed by Azize Bhaij, with resource support from Khalid Sabri and Redouane Jouali. Data management was coordinated by Azize Bhaij and Redouane Jouali. Writing-original draft preparation was done by Azize Bhaij, while writing-review and editing were jointly managed by Azize Bhaij and Abderrahim Haddad. Visualization was handled by Redouane Jouali. Project supervision was carried out by Mohssin

Aoutoul, with project administration ensured by Khalid Sabri. Finally, funding acquisition was managed by Mohssin Aoutoul.

## References


[1]. R. L. Siegel, A. N. Giaquinto, and A. Jemal, "Cancer statistics, 2024", *CA Cancer Journal for Clinicians*, Vol. 74, No. 1, 2024.

[2]. J. D. Emery *et al*., "The role of primary care in early detection and follow-up of cancer", *Nature Reviews Clinical Oncology*, Vol. 11, pp. 38-48, 2014.

[3]. D. Crosby *et al*., "Early detection of cancer", *Science*, Vol. 375, No. 6578, pp. 327-330, 2022.

[4]. M. Doroudi, R. E. Schoen, and P. F. Pinsky, "Early detection versus primary prevention in the PLCO flexible sigmoidoscopy screening trial: Which has the greatest impact on mortality?", *Cancer*, Vol. 123, No. 24, pp. 4832-4840, 2017.

[5]. R. Ramani, N. S. Vanitha, and S. Valarmathy, "The Pre-Processing Techniques for Breast Cancer Detection in Mammography Images", *International Journal of Image, Graphics and Signal Processing*, Vol. 5, No. 5, pp. 46-52, 2013.

[6]. H. Avcı and J. Karakaya, "A Novel Medical Image Enhancement Algorithm for Breast Cancer Detection on Mammography Images Using Machine Learning", *Diagnostics*, Vol. 13, No. 3, pp. 1-15, 2023.

[7]. H. Ben Pan, "The Role of Breast Ultrasound in Early Cancer Detection", *Journal of Medical Ultrasound*, Vol. 24, No. 4, pp. 199-204, 2016.

[8]. R. Sood *et al*., "Ultrasound for breast cancer detection globally: A systematic review and meta-analysis", *Journal of Global Oncology*, Vol. 2019, No. 5, pp. 1-16, 2019.

[9]. R. Guo, G. Lu, B. Qin, and B. Fei, "Ultrasound Imaging Technologies for Breast Cancer Detection and Management: A Review", *Ultrasound in Medicine and Biology*, Vol. 44, No. 1, pp. 37-70, 2018.

[10]. E. A. Morris, "Breast cancer imaging with MRI", *Radiologic Clinics of North America*, Vol. 40, No. 3, pp. 443-466, 2002.

[11]. C. K. Kuhl, "Abbreviated Magnetic Resonance Imaging (MRI) for breast cancer screening: Rationale, concept, and transfer to clinical practice", *Annual Review of Medicine*, Vol. 70, pp. 501-519, 2019.

[12]. N. Aristokli, I. Polycarpou, S. C. Themistocleous, D. Sophocleous, and I. Mamais, "Comparison of the diagnostic performance of Magnetic Resonance Imaging (MRI), ultrasound and mammography for detection of breast cancer based on tumor type, breast density and patient's history: A review", *Radiography*, Vol. 28, No. 2, pp. 204-213, 2022.

[13]. L. Pajewski *et al*., "Applications of Ground Penetrating Radar in Civil Engineering - COST action TU1208", In: *Proc. of the 2013 7th International Workshop on Advanced Ground Penetrating Radar*, pp. 145-152, 2013.

[14]. R. C. Daniels and R. W. Heath, "60 GHz wireless communications: Emerging requirements and design recommendations", *IEEE Vehicular Technology Magazine*, Vol. 2, No. 3, pp. 41-50, 2007.

[15]. M. A. Aldhaeebi, K. Alzoubi, T. S. Almoneef, S. M. Bamatra, H. Attia, and O. M. Ramahi, "Review of microwave techniques for breast cancer detection", *Sensors*, Vol. 20, No. 8, pp. 1-25, 2020.

[16]. C. Jr. Robert F., D. M. Sylvar, and J. L. Ulcek, "Evaluating compliance with FCC guidelines for human exposure to radiofrequency electromagnetic fields", *FCC OET Bulletin*, No. 65, pp. 1-36, 1997.

[17]. C. Kwok, R. F. Jr. Cleveland, and D. L. Means, "Evaluating Compliance with FCC Guidelines for Human Exposure to Radiofrequency Electromagnetic Fields Supplement C", *Federal Communications Commission Office of Engineering & Technology*, Vol. 65, pp. 1-24, 2001.

[18]. R. Natarajan, J. V. George, M. Kanagasabai, and A. Kumar Shrivastav, "A Compact Antipodal Vivaldi Antenna for UWB Applications", *IEEE Antennas and Wireless Propagation Letters*, Vol. 14, pp. 1284-1287, 2015.

[19]. R. Natarajan, M. Gulam Nabi Alsath, M. Kanagasabai, S. Bilvam, and S. Meiyalagan, "Integrated Vivaldi antenna for UWB/diversity applications in vehicular environment", *International Journal of RF and Microwave Computer-Aided Engineering*, Vol. 30, No. 1, pp. 1-10, 2020.

[20]. M. Moosazadeh, S. Kharkovsky, and J. T. Case, "Microwave and millimeter wave antipodal Vivaldi antenna with trapezoid-shaped dielectric lens for imaging of construction materials", *IET Microwaves*, Antennas & Propagation, Vol. 10, No. 3, pp. 279-285, 2016.

[21]. S. Guruswamy, R. Chinniah, and K. Thangavelu, "Design and implementation of compact ultra-wideband Vivaldi antenna with directors for microwave-based imaging of breast cancer",

*Analog Integrated Circuits and Signal Processing*, Vol. 108, No. 1, pp. 95-106, 2021.

[22]. S. Guruswamy, R. Chinniah, and K. Thangavelu, "A printed compact UWB Vivaldi antenna with hemi cylindrical slots and directors for microwave imaging applications", *AEU - International Journal of Electronics and Communications*, Vol. 110, pp. 1-9, 2019.

[23]. D. N. Elsheakh and E. A. Abdallah, "Compact ultra-wideband Vivaldi antenna for ground-penetrating radar detection applications", *Microwave and Optical Technology Letters*, Vol. 61, No. 5, pp. 1285-1290, 2019.

[24]. S. Saleh, M. H. Jamaluddin, B. Alali, and A. A. Althuwayb, "Compact 5G Vivaldi Tapered Slot Filtering Antenna with Enhanced Bandwidth", *Computers, Materials & Continua*, Vol. 74, No. 3, pp. 5661-5673, 2023.

[25]. A. S. Dixit and S. Kumar, "Gain Enhancement of Antipodal Vivaldi Antenna for 5G Applications Using Metamaterial", *Wireless Personal Communications*, Vol. 121, No. 4, pp. 2349-2361, 2021.

[26]. E. W. Reid, L. O - Balbuena, A. Ghadiri, and K. Moez, "A 324-element Vivaldi antenna array for radio astronomy instrumentation", *IEEE Transactions on Instrumentation and Measurement*, Vol. 61, No. 1, pp. 56-63, 2012.

[27]. S. Saleh, M. H. Jamaluddin, F. Razzaz, S. M. Saeed, N. Timmons, and J. Morrison, "Compactness and performance enhancement techniques of ultra-wideband tapered slot antenna: A comprehensive review", *Alexandria Engineering Journal*, Vol. 62, pp. 23-34, 2023.

[28]. S. Tangwachirapan, W. Thaiwirot, and P. Akkaraekthalin, "Design and Analysis of Antipodal Vivaldi Antennas for Breast Cancer Detection", *Computers, Materials & Continua*, Vol. 73, No. 1, pp. 411-431, 2022.

[29]. P. J. Gibson, "VIVALDI AERIAL.", In: *Proc. of the European Microwave Conference*, pp. 101-105, 1979.

[30]. M. T. Islam, M. Z. Mahmud, N. Misran, J. I. Takada, and M. Cho, "Microwave Breast Phantom Measurement System with Compact Side Slotted Directional Antenna", *IEEE Access*, Vol. 5, pp. 5508-5516, 2017.

[31]. G. V. Krishna, B. T. P. Madhav, M. V. Giridhar, M. V. Reddiah Babu, V. Sai Krishna, and S. S. Mohan Reddy, "Bandwidth enhanced antipodal Vivaldi antenna for wide band communication applications", *Indian Journal of Science and Technology*, Vol. 9, No. 31, pp. 1-9, 2016.

[32]. A. M. Qashlan, R. W. Aldhaheri, and K. H. Alharbi, "A Modified Compact Flexible Vivaldi Antenna Array Design for Microwave Breast Cancer Detection", *Applied Sciences*, Vol. 12, No. 10, pp. 4908-4917, 2022.

[33]. E. R. Alagee and A. Assalem, "Brain Cancer Detection Using U-Shaped Slot VIVALDI Antenna and Confocal Radar Based Microwave Imaging Algorithm", *American Scientific Research Journal for Engineering*, Technology, and Sciences, Vol. 66, No. 1, pp. 1-12, 2020.

[34]. S. Sasikala, K. Karthika, S. Arunkumar, K. Anusha, S. Adithya, and A. J. A. Al-Gburi, "Design and analysis of a low-profile tapered slot UWB Vivaldi antenna for breast cancer diagnosis", *Progress in Electromagnetics Research M*, Vol. 124, pp. 43-51, 2024.

[35]. A. T. G. Abouelnaga and A. F. Desouky, "UWB Antenna with All Band Suitable Radiation Pattern for Breast Cancer Detection", *International Journal of Engineering and Technology*, Vol. 9, No. 2, pp. 720-726, 2017.